Atmos. Meas. Tech., 8, 2639–2648, 2015
www.atmos-meas-tech.net/8/2639/2015/
doi:10.5194/amt-8-2639-2015

Atmospheric Measurement Techniques
Open Access

Measurement of carbonaceous aerosol with different sampling configurations and frequencies

Y. Cheng[1] **and K.-B. He**[1,2,3]

[1]State Key Joint Laboratory of Environment Simulation and Pollution Control, School of Environment, Tsinghua University, Beijing, China
[2]State Environmental Protection Key Laboratory of Sources and Control of Air Pollution Complex, Beijing, China
[3]Collaborative Innovation Center for Regional Environmental Quality, Beijing, China

Correspondence to: K.-B. He (ycheng@mail.tsinghua.edu.cn, hekb@tsinghua.edu.cn)

Received: 08 December 2014 – Published in Atmos. Meas. Tech. Discuss.: 20 March 2015
Revised: 09 June 2015 – Accepted: 17 June 2015 – Published: 01 July 2015

Abstract. A common approach for measuring the mass of organic carbon (OC) and elemental carbon (EC) in airborne particulate matter involves collection on a quartz fiber filter and subsequent thermal–optical analysis. Although having been widely used in aerosol studies and in $PM_{2.5}$ (fine particulate matter) chemical speciation monitoring networks in particular, this measurement approach is prone to several types of artifacts, such as the positive sampling artifact caused by the adsorption of gaseous organic compounds onto the quartz filter, the negative sampling artifact due to the evaporation of OC from the collected particles and the analytical artifact in the thermal–optical determination of OC and EC (which is strongly associated with the transformation of OC into char OC and typically results in an underestimation of EC). The presence of these artifacts introduces substantial uncertainties to observational data on OC and EC and consequently limits our ability to evaluate OC and EC estimations in air quality models. In this study, the influence of sampling frequency on the measurement of OC and EC was investigated based on $PM_{2.5}$ samples collected in Beijing, China. Our results suggest that the negative sampling artifact of a bare quartz filter could be remarkably enhanced due to the uptake of water vapor by the filter medium. We also demonstrate that increasing sampling duration does not necessarily reduce the impact of positive sampling artifact, although it will enhance the analytical artifact. Due to the effect of the analytical artifact, EC concentrations of 48 h averaged samples were about 15 % lower than results from 24 h averaged ones. In addition, it was found that with the increase of sampling duration, EC results exhibited a stronger dependence on the charring correction method and, meanwhile, optical attenuation (ATN) of EC (retrieved from the carbon analyzer) was more significantly biased by the shadowing effect. Results from this study will be useful for the design of China's $PM_{2.5}$ chemical speciation monitoring network, which can be expected to be inaugurated in the near future.

1 Introduction

Particulate matter (PM) pollution has become a substantial concern in China. Through the air quality management practice during the last 2 decades, both the scientific community and the Chinese government have recognized that the emissions of not only primary PM but also gaseous precursors of PM must be reduced to control the PM pollution (Wang et al., 2010). However, each step along the way between source and atmospheric concentration of PM is still rather complex. Even for secondary inorganic aerosol, the formation mechanisms of which have been relatively well characterized, there might be a large gap between simulation results and observational data (e.g., Zheng et al., 2015). Compared to observations performed by individual research groups, information derived from large-scale PM monitoring networks is more suitable for evaluating air quality models as well as other techniques such as satellite remote sensing (Koch et al., 2009; Jathar et al., 2011; Boys et al., 2014). For example, global $PM_{2.5}$ (fine particulate matter) composition inferred from remote sensing in combination with modeling was as-

sessed by the observational data from three networks, including the Interagency Monitoring of Protected Visual Environments (IMPROVE) network in the United States, the European Monitoring and Evaluation Programme (EMEP) network and the National Air Pollution Surveillance (NAPS) network in Canada (Philip et al., 2014). In China, the Ministry of Environmental Protection (MEP) has started to establish a $PM_{2.5}$ monitoring network on a national scale. The network now provides hourly averaged mass concentrations of $PM_{2.5}$ for 190 cites, which have been shown to be useful for evaluating $PM_{2.5}$ predictions from air quality models (e.g., Zheng et al., 2015). Compared to those in North America and Europe, however, the $PM_{2.5}$ network in China is still at the initial stage mainly due to the lack of speciation measurements. Therefore, a good understanding of the speciation measurements, especially the uncertainties associated with sampling and analytical procedures, is highly desirable in China.

In general, $PM_{2.5}$ is a complex mixture of carbonaceous components (including organic carbon (OC) and elemental carbon (EC)), water-soluble inorganic ions, trace elements and crustal materials. These species possess a wide range of properties such as volatility and solubility and, thus, require different sampling and analytical techniques. At present, the challenges mainly come from the carbonaceous components (Turpin et al., 2000; US EPA, 2004; Malm et al., 2011; Solomon et al., 2014).

A common approach for measuring the mass of OC and EC in airborne particles involves collection on a quartz filter and subsequent thermal–optical analysis. As for sampling, there exist two types of artifacts. One is the positive artifact due to the adsorption of gaseous organic compounds onto the quartz filter, while the other one is the negative artifact caused by the evaporation of OC from the collected particles. Sampling artifacts will lead to an overestimation or underestimation of OC concentrations depending on whether the main artifact is adsorption (of gaseous organics) or evaporation (of particulate OC). One way to correct for the positive artifact is to introduce a backup quartz filter (placed downstream of either the primary quartz filter or a Teflon filter collected in parallel with the primary quartz filter) and use its OC content as a measure of the positive artifact on the primary quartz filter. An alternative method to eliminate the positive artifact is adding a denuder capable of removing gaseous organics upstream of the sampling filter. Moreover, if a denuder is placed upstream of a filter pack, OC measured by the denuded backup filter will provide an estimation of the negative artifact. In the $PM_{2.5}$ networks in North America and Europe, the positive artifact has not been well addressed yet, while the negative artifact is usually left unaccounted for (Watson et al., 2009; Maimone et al., 2011; Solomon et al., 2014). When only focusing on the positive artifact, the backup quartz filter approach is much simpler than the denuder approach (e.g., with respect to sampler operation), although it usually either overestimates or underestimates the positive artifact (Eatough et al., 2003; Subramanian et al., 2004; Viana et al., 2006; Cheng et al., 2010).

As for thermal–optical analysis, EC can survive up to ~ 900 K in the presence of oxygen and, meanwhile, the removal (e.g., combustion) of EC leads to a rapid increase of the filter transmittance and reflectance signals which are typically monitored at 632 or 678 nm (Chow et al., 2004; Cavalli et al., 2010). Thus, EC is distinguished from OC by its much higher thermal stability and considerably stronger light-absorbing capacity in the spectral range of red light. A major problem in thermal–optical methods is that a substantial fraction of organic species can be transformed into materials whose thermal and optical behaviors are quite similar to EC (these materials are typically termed char OC or pyrolysis OC), thus affecting the separation of OC and EC (Yang and Yu, 2002; Chow et al., 2004; Subramanian et al., 2006). A variety of studies have shown that thermal–optical determination of OC and EC depends strongly on the analytical procedure such as the temperature protocol and the charring correction method (Chow et al., 2001, 2004; Schmid et al., 2001; Schauer et al., 2003; ten Brink et al., 2004; Cavalli et al., 2010; Chiappini et al., 2014; Panteliadis et al., 2015); moreover, the dependence is significantly influenced by sample properties such as source of carbonaceous components and abundance of minerals.

The spatial and temporal variations of the $PM_{2.5}$ composition in China are far from being well characterized, indicating that a national $PM_{2.5}$ speciation monitoring network is necessary. Compared to the sampling schedule used by established networks such as IMPROVE and NAPS (24 h samples are collected every 3 days), low-frequency, long-duration sampling is an alternative choice for China, which might be more suitable for a general perspective of the $PM_{2.5}$ composition on a national scale. Therefore, in this study we focus on the influence of sampling frequency (i.e., duration) on the measurement of carbonaceous aerosol. It is commonly believed that increasing sampling duration can reduce the influence of the positive sampling artifact and meanwhile does not affect the EC measurement (e.g., Subramanian et al., 2004). Here we demonstrate that this is not necessarily the case. Results from this study will be useful for the design of China's $PM_{2.5}$ speciation monitoring network, which can be expected to be inaugurated in the near future.

2 Methods

2.1 Field sampling

Ambient $PM_{2.5}$ samples were collected on the campus of Tsinghua University during the summer of 2009 (from 20 June to 20 July). Tsinghua University (40.00° N, 116.32° E) is located in the urban area of Beijing, about 20 km northwest of the city center. There is a main road with heavy traffic (i.e., the 4th Ring Road) about 1 km south of the campus, whereas

Table 1. Configuration of the SASS sampler (only the three channels used in this study are shown). Samples from channels 1 and 2, which are collected at a relatively high frequency, are referred to as high-frequency samples for simplicity; correspondingly, samples from channel 3 are termed low-frequency ones. This does not necessarily mean that 24 h averaged sampling should be considered as high-frequency sampling elsewhere.

Channel	1 (high frequency)	2 (high frequency)	3 (low frequency)
Denuder	Activated carbon	NA	NA
Front filter	Quartz (DQ)	Quartz (BQ)	Quartz (BQ)
Backup filter	Quartz (D-QBQ)	Quartz (QBQ)	Quartz (QBQ)
Sampling duration	~ 24 h[a]	~ 24 h[a]	~ 48 h[b]

[a] It took about 1 h to change filters and maintain the sampler for each set of sample; thus, the sampling duration is not exactly 24 h for channels 1 and 2. However, samples collected by these two channels will still be termed daily samples or 24 h samples.
[b] During each sampling event of channel 3, there is a period when channels 1 and 2 were stopped for filter change. Channel 3 was also stopped in this period.

there are no major industrial sources nearby. The sampling was done by a Spiral Ambient Speciation Sampler (SASS; Met One Instruments, OR, USA) with five separate channels operated through a common pump. The sampling flow rate was 6.7 L min^{-1} for each channel, corresponding to a cut-point of 2.5 µm (given by a sharp cut cyclone). The sampler was placed on the roof a building on the campus, about 6 m above the ground.

Three channels with sequential quartz filters were used in the present study and their configurations are summarized in Table 1. Channels 1 and 2 were operated at a relatively high frequency with a sampling duration of 24 h, while channel 3 was run at a relatively low frequency such that the sampling duration was 48 h. In channel 1, an activated carbon denuder (Met One Instruments, OR, USA) was placed upstream of the sequential quartz filters to remove gaseous organics and thus eliminate the positive sampling artifact. The activated carbon denuder was 20 mm long and 38 mm in diameter with about 1000 1 mm × 1 mm channels. At the operating flow rate (6.7 L min^{-1}), the residence time of particles in the denuder was about 0.18 s. The same denuder was used throughout the measurement period. Evaluation of the denuder has been presented elsewhere (Cheng et al., 2010) and is also available in the Supplement. The quartz filters (8 in × 10 in, 2500 QAT-UP; Pall Corporation, NY, USA) were taken from the same lot, first cut into punches with a diameter of 47 mm and then baked at 550 °C in air for 24 h before use.

2.2 Sample analysis

The quartz filters were analyzed for OC and EC using a DRI carbon analyzer (Model 2001; Atmoslytic Inc., CA, USA). The temperature protocol implemented was IMPROVE-A, which heats the sample in an inert (i.e., He; up to 580 °C) and oxidizing (i.e., He / O_2; up to 840 °C) atmosphere sequentially. Both the transmittance and reflectance charring corrections were used to separate OC and EC. In the transmittance correction approach, EC is defined as the carbon evolving after the filter transmittance signal (monitored at a wavelength of 632 nm) returns to its initial value, whereas the reflectance correction defines EC based on the reflectance signal (also monitored at 632 nm). Without special statement, all of the OC and EC results reported in this article are based on the transmittance charring correction and have been corrected by the filter blank concentrations (blank OC averaged 0.43 ± 0.12 µgC cm^{-2}, whereas no blank EC was detected; a total of 15 blank filters were collected).

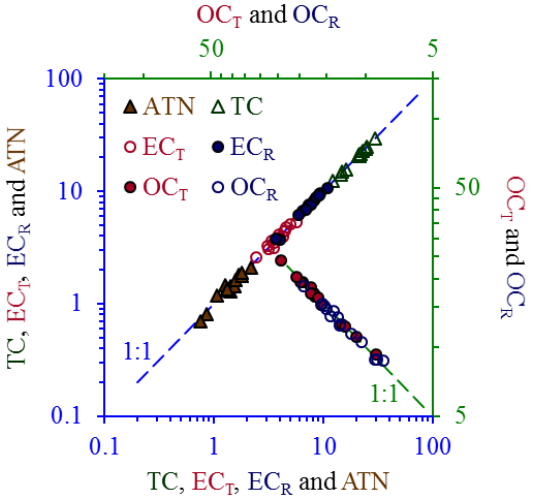

Figure 1. Comparison of the carbon (i.e., TC, OC and EC) and optical (i.e., ATN) measurements performed by duplicate analysis. TC, OC and EC are presented in µgC cm^{-2}. The subscripts "R" and "T" indicate reflectance- and transmittance-based charring correction, respectively.

2.3 Equipment performance

The sampling flow rate of the SASS sampler averaged 6.73 ± 0.02, 6.72 ± 0.01 and 6.72 ± 0.01 L min^{-1} for the three channels used in this study. Thus, the sampling flow rate was stable for each channel and agreed well among different channels.

The performance of the DRI carbon analyzer is demonstrated in Fig. 1. Duplicate analysis suggested good precision for the carbon (i.e., total carbon (TC), OC and EC) and optical (i.e., optical attenuation (ATN)) measurements, both of which were within 5 %. The precision was evaluated as the ratio of the standard deviation of the duplicate measurements to the average value. Optical ATN is calculated as

$$\mathrm{ATN} = \ln\left(\frac{T_{\mathrm{final}}}{T_{\mathrm{initial}}}\right), \quad (1)$$

where T_{initial} and T_{final} are the intensity of the transmittance signal measured at the beginning (i.e., when the loaded filter has not been heated) and end (i.e., when all of the loaded carbon has been combusted off the filter) of thermal–optical analysis, respectively. ATN provides an estimation of the light absorption due to the loaded particles (Ram and Sarin, 2009), although with artifacts (e.g., those caused by the aerosol-filter interactions and filter scattering). The measurement of ATN by the DRI carbon analyzer was similar to that by the filter-based online instruments such as the Aethalometer and the Particle Soot/Absorption Photometer. These online instruments typically measure the transmittance signal across a loaded (T_{loaded}) and a particle-free reference filter ($T_{\mathrm{reference}}$) simultaneously, while ATN is calculated as

$$\mathrm{ATN} = \ln\left(\frac{T_{\mathrm{reference}}}{T_{\mathrm{loaded}}}\right). \quad (2)$$

T_{loaded} and $T_{\mathrm{reference}}$ in Eq. (2) are equivalent to T_{initial} and T_{final} in Eq. (1), respectively. Thus, ATN retrieved from the DRI carbon analyzer is comparable to that given by the filter-based, online instruments. However, the comparison may not be straight forward in practice (e.g., the measurement wavelength could be different). Refer to the Supplement for a more detailed discussion regarding this point, which goes beyond the scopes of this paper. The Supplement also includes a summary of the statistical results for the comparisons, regressions and ratios included in this paper (e.g., the comparisons shown in Fig. 1).

2.4 Meteorological information

Meteorological parameters for Beijing during this study were obtained from Weather Underground (http://www.wunderground.com/global/stations/54511.html), which were measured at the Beijing International Airport (40.07° N, 116.59° E). The average temperature and relative humidity (RH) for each sample collection period were calculated by averaging the raw data (with a time resolution of 30 min) according to the start and stop time of each sampling event. The meteorological information was mainly used to identify a distinct period with high RH levels. The identification result was strongly supported by the RH data from another source (the China Meteorological Data Sharing Service System; see the Supplement).

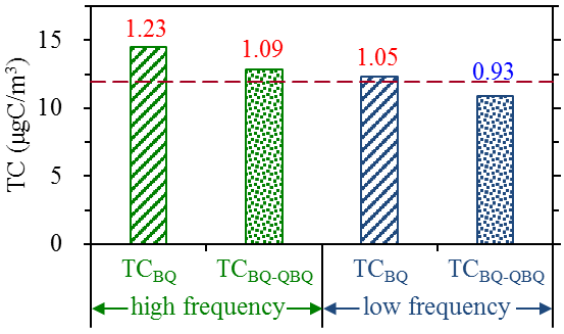

Figure 2. Comparison of the 48 h averaged TC concentrations measured by different sampling configurations and frequencies. The dashed line corresponds to the reference value, which is the average of the TC concentrations measured by the high-frequency denuded filters (i.e., DQ). The bars indicate the alternative TC estimations. The values above each bar are the average of the alternative-to-reference ratios, while the red and blue fonts indicate an overestimation and underestimation, respectively.

3 Results and discussion

3.1 Effect of sampling frequency on the sampling artifacts

In this study, 48 h averaged TC rather than OC concentrations are used to investigate the sampling artifacts. This is because the discrepancies in OC results measured by different sampling frequencies are also affected by the analytical artifact besides the sampling artifacts (this point will be discussed in Sect. 3.2), whereas TC results are not. Nonetheless, it has been shown that (i) the activated carbon denuder used in this study could completely remove the positive artifact and did not bias the EC measurement, and (ii) negligible OC could be detected on the denuded backup quartz filter (D-QBQ; Table 1) throughout this study (Cheng et al., 2010; also see the Supplement). Therefore, 48 h averaged TC measured by the denuded front quartz filter (DQ; Table 1) is used as the reference value.

Figure 2 compares the 48 h averaged TC concentrations measured by different sampling configurations and frequencies. As for the high-frequency samples, TC concentrations of the bare quartz filters (high-frequency $\mathrm{TC_{BQ}}$) were 23 % higher than those of the denuded ones (high-frequency $\mathrm{TC_{DQ}}$), indicating a significant positive artifact. OC measured by the backup quartz filter was used to account for the positive artifact; however, the corrected results (high-frequency $\mathrm{TC_{BQ-QBQ}}$) still overestimated TC by 9 %, indicating that the backup filter adsorbed less gaseous organics compared to the front one. With respect to the low-frequency samples, TC concentrations (low-frequency $\mathrm{TC_{BQ}}$) were only 5 % higher than the reference values (i.e., the high-frequency $\mathrm{TC_{DQ}}$). Previous studies conducted at Berkeley, CA, and the Pittsburgh Air Quality Study (PAQS) supersite

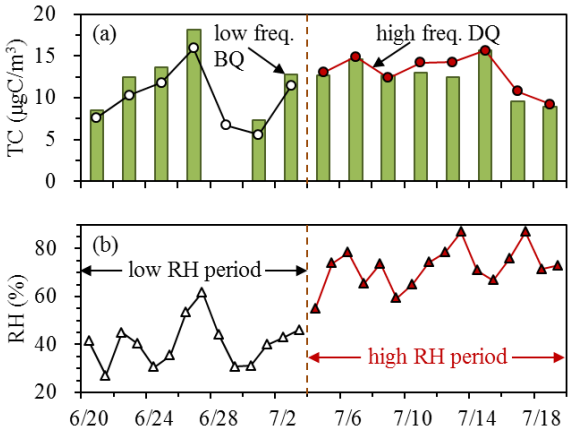

Figure 3. Temporal variations of TC concentration (48 h averages) and RH (24 h averages). RH averaged 41 ± 10 and 72 ± 9 % during the low RH and high RH periods, respectively; the difference is significant at a 95 % level of confidence (two-tailed $p = 0.000$). The identification of the high RH period is also supported by RH data from another source (i.e., the China Meteorological Data Sharing Service System; see the Supplement).

also showed that the positive artifact was less significant for low-frequency samples (Kirchstetter et al., 2001; Subramanian et al., 2004). It seems that increasing the sampling duration could remarkably reduce the influence of the positive artifact even more effectively than introducing a backup filter. A possible explanation for this phenomenon is suggested to be that a low-frequency quartz filter is more likely to reach equilibrium with gaseous organics due to its relatively long sampling duration. Once the equilibrium has been reached, the artifact mass on the filter stops to increase and remains constant with increasing sampling time (Subramanian et al., 2004).

It has been well documented that TC concentration measured by a bare quartz filter will be more or less reduced by placing a denuder upstream. As shown in Fig. 3a, however, the low-frequency TC_{BQ} was lower than the high-frequency TC_{DQ} for several data points (the difference was significant at a 95 % level of confidence; two-tailed $p = 0.044$), although the low-frequency TC_{BQ} was higher in terms of average concentration (Fig. 2). This phenomenon has not been observed before. The high-frequency TC_{DQ} was expected to provide a minimum estimation of the 48 h averaged TC concentration, because (i) the positive artifact had been removed by the charcoal denuder with an efficiency of 100 %, and (ii) the negative artifact was enhanced since the denuder disturbed the gas-particle equilibrium of semivolatile organic compounds. Thus, it is really surprising that the low-frequency TC_{BQ}, which should be biased high due to the positive artifact, could be lower than the high-frequency TC_{DQ}. The only explanation is that the negative artifact could be more significant for the low-frequency samples than the denuded ones, meaning that the comparisons shown in Fig. 2 do not necessarily indicate that the positive sampling artifact is less significant for the low-frequency samples. Factors responsible for these unexpected higher negative artifacts of the low-frequency samples are discussed below.

We first investigated the effects of temperature. As mentioned in the Methods section, the sampling period of a low-frequency filter included two non-overlapping segments, corresponding to two high-frequency samples. If the temperature was higher during the second segment, particulate carbon collected during the first one was subject to additional loss for the low-frequency samples, resulting in a greater negative artifact. With respect to the sampling events when the low-frequency TC_{BQ} was lower than the high-frequency TC_{DQ} ($N = 8$), only 50 % were found to have a higher temperature during the second segment. Moreover, a higher temperature during the second segment could also be observed in the remaining sampling events (i.e., when the low-frequency TC_{BQ} were higher than the reference values). Therefore, daily variation in temperature is not a likely cause of the unexpected higher negative artifacts of the low-frequency samples.

We then investigated the effects of filter loading. The pressure drop across a sampling filter increases as particles are collected, providing a driving force for the loss of particulate carbon (Turpin et al., 2000). Higher pressure drop is expected to make the negative artifact more significant. For example, it is well known that Teflon filters are more susceptible to the negative artifact than quartz filters due to their higher pressure drop (Turpin et al., 1994). Compared to the high-frequency samples, the low-frequency ones had a much higher particle loading per filter, resulting in a much higher pressure drop which consequently enhances the negative artifact. However, it seems that filter loading was not the only factor responsible for the unexpected higher negative artifacts of the low-frequency samples. This is because the occurrence of these unexpected higher negative artifacts did not exhibit an apparent dependence on the filter loading of the low-frequency samples. For example, during the sampling period with the highest 48 h integrated TC loading (i.e., with the highest 48 h averaged TC concentration), the low-frequency TC_{BQ} (18.10 $\mu gC\,m^{-3}$) was substantially higher than the high-frequency TC_{DQ} (15.92 $\mu gC\,m^{-3}$), showing no solid evidence for a greater negative artifact being associated with the low-frequency filter (Fig. 3a). Therefore, in addition to the effect of filter loading, there must exist other factors that are able to strongly enhance the negative artifact of the low-frequency filters.

Interestingly, all of the lower levels of the low-frequency TC_{BQ}, relative to the reference values, were observed during a period characterized by high RH (Fig. 3b). Unlike particle-bound water, gas-phase water in the atmosphere is typically not considered as a biasing factor during aerosol measurements (US EPA, 2004). However, some types of sampling filters, such as quartz, are indeed able to adsorb water vapor (Brown et al., 2006). In a previous study conducted in the

Netherlands, a blank quartz filter (with a diameter of 47 mm), which was kept in a weighing room as a laboratory reference for the gravimetric measurement of PM mass, exhibited a slowly increasing mass of almost 500 µg over ∼ 1500 days due to the adsorption of gas-phase water (de Jonge and Visser, 2009). Similar to the collected particles, the adsorbed water vapor also contributes to the pressure drop across a sampling filter (Liew and Conder, 1985). Thus, the negative artifact (of a bare quartz filter) is expected to be more significant under high RH conditions. However, it is well known that activated carbon can adsorb water vapor (Müller et al., 1996), suggesting that the charcoal denuder used in this study was able to reduce the abundance of gas-phase water in the sampling follow (although with an unknown efficiency). Consequently, the uptake of water vapor by the denuded filters was less significant compared to the bare ones, leading to a lower pressure drop which tends to reduce the negative artifact. Importantly, the unexpected higher negative artifacts of the low-frequency samples occurred only in the high RH period, demonstrating that the uptake of water vapor by the filter medium can greatly enhance the loss of particulate carbon. During the high RH period, the low-frequency TC_{BQ} underestimated TC concentration by 5 %, while TC was further underestimated (by 16 %) if the low-frequency TC_{BQ} was corrected for the positive artifact (the corrected results are referred to as the low-frequency TC_{BQ-QBQ}; Fig. 4a).

Figure 4 also compares the high-frequency TC_{BQ} and TC_{BQ-QBQ} with the reference values. Compared to results from the low RH period, overestimation of TC by the high-frequency TC_{BQ} was less significant during the high RH period while the high-frequency TC_{BQ-QBQ} was more comparable with the reference value. Traditionally, these results would be attributed to a smaller positive artifact during the high RH period and a better performance of the quartz-quartz in series method. However, we suggest that there is another possible explanation: compared to the denuded one, the bare quartz filter was biased by a greater negative artifact during the high RH period. Therefore, the uptake of water vapor by the bare quartz filter can complicate our understandings of the positive artifact through enhancing the negative artifact, especially under high RH conditions.

It should be mentioned that here we assume the adsorption of gas-phase water by the collected particles is not important, since particle-bound water is presumably in equilibrium with the gas phase at the time of collection. Similarly, it was suggested that the collected particles did not contribute significantly to the adsorption of gaseous organics (McDow and Huntzicker, 1990).

3.2 Effect of sampling frequency on the analytical artifact

When both of them were collected at the high frequency, 48 h averaged EC concentrations agreed well between the denuded and un-denuded filters; however, substantially lower

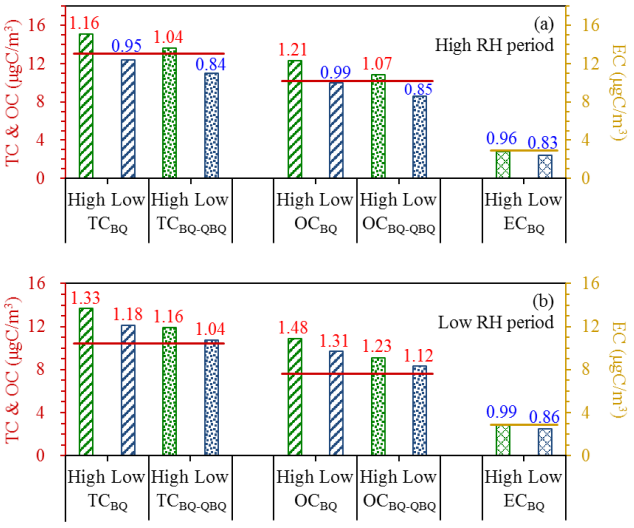

Figure 4. Comparison of the 48 h averaged TC, OC and EC concentrations measured by different sampling configurations and frequencies during the high RH **(a)** and low RH **(b)** periods. In the title of each horizontal axis, "High" and "Low" indicate results from the high- and low-frequency samples, respectively. The horizontal lines correspond to the reference values, which are derived from the high-frequency denuded filters (i.e., DQ). The bars indicate the alternative estimations. The values above each bar are the average of the alternative-to-reference ratios, while the red and blue fonts indicate an overestimation and underestimation, respectively. The difference between the high-frequency EC_{BQ} and the reference value (i.e., the high-frequency EC_{DQ}) is not significant at a 95 % level of confidence (two-tailed $p = 0.113$), whereas the difference between the low-frequency EC_{BQ} and the reference value is significant (two-tailed $p = 0.000$). Scatter plots describing the comparisons shown in this figure are provided in the Supplement.

values (by about 15 %) were measured by the low-frequency samples (Fig. 4), consistent with results from a suburban site in Europe (Chiappini et al., 2014). Although the EC measurement is not susceptible to sampling artifacts, thermal–optical determination of EC could be largely complicated by the transformation of OC into char OC (Yang and Yu, 2002). It has been demonstrated that thermal–optical methods tend to underestimate EC (i.e., overestimate OC) due to uncertainties associated with the separation of char OC and EC, resulting in the analytical artifact (Chow et al., 2004; Subramanian et al., 2006). In a previous study conducted in Beijing, China, the formation of char OC was reduced by extracting the filters using a mixture of hexane, methylene chloride and acetone (about 55 % of OC was removed in this way), and a 6 % increase in the EC results was observed after the extraction (Cheng et al., 2012). EC results were also found to increase after the filters collected in Milan, Italy, were washed by water (Piazzalunga et al., 2011). These results suggest that the analytical artifact tends to be reduced as less char OC is formed, or, in other words, the analytical artifact tends to be enhanced as more char OC is formed. The amount of char

OC per filter, which was roughly proportional to the filter's OC loading, was much higher for the low-frequency samples compared to the high-frequency ones. Thus, the underestimation of EC (i.e., the overestimation of OC) caused by the analytical artifact was more significant for the low-frequency samples, which is responsible for their lower EC concentrations compared to the high-frequency filters (Fig. 4).

Influences of sampling frequency on the 48 h averaged OC concentrations were in general similar to those observed in the comparison of TC results (Fig. 4). Briefly, OC concentrations of the low-frequency filters (low-frequency OC_{BQ}) were always lower than those measured by the high-frequency un-denuded ones (high-frequency OC_{BQ}) regardless of the RH levels. Compared to results from the high-frequency denuded samples (high-frequency OC_{DQ}), the low-frequency OC_{BQ} was higher (by 31 %) during the low RH period, whereas it was 1 % lower during the high RH period (due to a greater negative artifact). As mentioned above, the overestimation of OC caused by the analytical artifact was more significant for the low-frequency samples, indicating that the OC comparisons shown in Fig. 4 were affected by not only the sampling artifacts but also the analytical artifact. For example, if only considering the influences of the sampling artifacts, the low-frequency OC_{BQ} should be lower than the high-frequency OC_{DQ} by more than 5 % during the high RH period (5 % corresponded to the difference between the low-frequency TC_{BQ} and the high-frequency TC_{DQ} during the same period; Fig. 4a), whereas the difference was reduced to 1 % after accounting for the analytical artifact.

3.3 Effect of sampling frequency on the optical attenuation measurement

ATN is of interest because it can be used to calculate the absorption coefficient (b_{abs}) and the mass absorption efficiency (MAE) of black carbon (Ram and Sarin, 2009), two parameters of great interest in the climate community:

$$b_{abs}\left(\mathrm{Mm}^{-1}\right) = \mathrm{ATN} \times \frac{A}{V}, \tag{3}$$

$$\mathrm{MAE}\left(\mathrm{m}^2\,\mathrm{g}^{-1}\right) = \frac{b_{abs}}{\mathrm{EC_m}} = \frac{\mathrm{ATN}}{\mathrm{EC}_s} \times 100, \tag{4}$$

where A is the filter area with particle loading (mm^2), V is the volume of air sampled (m^3), EC_m is the mass concentration of EC ($\mu g\,m^{-3}$) and EC_s indicates the EC loading ($\mu g\,cm^{-2}$). As shown in Eq. (4), ATN is related to EC loading, rather than EC concentration. Therefore, the comparison of ATN between the high- and low-frequency samples is performed based on the 48 h integrated values.

As shown in Fig. 5, ATN measured by the low-frequency filters (low-frequency ATN_{BQ}) were about 10 % lower than the integrated values of the high-frequency denuded samples (integrated high-frequency ATN_{DQ}). This difference

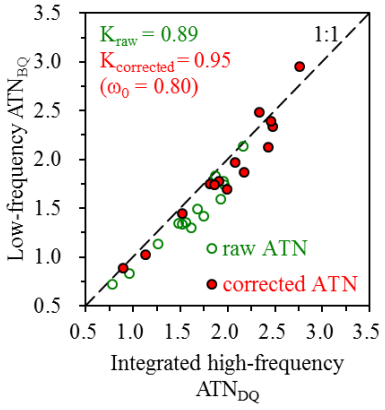

Figure 5. Comparison of the low-frequency ATN_{BQ} and the integrated high-frequency ATN_{DQ}. The comparison is performed based on both the uncorrected and corrected ATN. The correction is made by Eqs. (5)–(7) in which ω_0 is assumed to be 0.80. The correction has also been made by assuming $\omega_0 = 0.85$ and 0.90, but the results are not presented here. Linear regression results are shown with K as slope (intercept is set as 0). For the uncorrected ATN results, the difference between the low-frequency ATN_{BQ} and the integrated high-frequency ATN_{DQ} is significant at a 95 % level of confidence (two-tailed $p = 0.000$).

was caused by the shadowing effect (also known as the loading effect), which means that an increased underestimation of ATN occurs with increasing filter loadings (Weingartner et al., 2003). The shadowing effect was also observed in a previous study with two aethalometers being operated in parallel such that the Aethalometer with the most recent filter change (i.e., with a relatively low filter loading) always gave higher readings than the other (i.e., the Aethalometer with a relatively high filter loading) until the other instrument's filter change (LaRosa et al., 2002). Schmid et al. (2006) attributed the shadowing effect to the decrease in the ATN measurement sensitivity with increasing filter loadings. A correction factor, R(ATN), was introduced by Weingartner et al. (2003) to account for the shadowing effect:

$$\mathrm{ATN}^* = \frac{\text{raw ATN}}{R\,(\mathrm{ATN})}, \tag{5}$$

$$R\,(\mathrm{ATN}) = \left(\frac{1}{f} - 1\right) \times \frac{\ln(\mathrm{ATN}) - \ln(10\,\%)}{\ln(50\,\%) - \ln(10\,\%)} + 1, \tag{6}$$

$$f = m \times (1 - \omega_0) + 1, \tag{7}$$

where ATN^* indicates the ATN result that has been corrected for the shadowing effect, ω_0 is the single scattering albedo and m is nearly a constant which was estimated to be 0.87 and 0.85 at a wavelength of 450 and 660 nm, respectively. ATN = 10 % is taken as a reference point. If the measured ATN ≤ 10 %, the loading effect is negligible and R(ATN)

is set to unity. However, if the measured ATN > 10 %, the shadowing effect should be corrected and R(ATN) becomes smaller than unity. The minimum ATN value was about 0.2 and 0.7 for the high- and low-frequency filters, respectively, indicating that a correction for the shadowing effect was necessary for both of them. Although ω_0 was not measured in this study, previous studies conducted in Beijing, China, suggested that its value was between 0.8 and 0.9 for the urban area (e.g., Eck et al., 2005; He et al., 2009). We tried to account for the shadowing effect through Eqs. (5)–(7) by assuming a ω_0 value and found that the agreement between the low-frequency ATN_{BQ} and the integrated high-frequency ATN_{DQ} was improved after the correction. Their difference was reduced to 8, 6 and 5 %, respectively, when assuming $\omega_0 = 0.90$, 0.85 and 0.80 (Fig. 5).

In addition to the shadowing effect, another artifact biasing the filter-based ATN measurement is the multiple scattering effect which results in an overestimation of ATN. Weingartner et al. (2003) introduced an empirical constant C to account for this artifact. Finally, the corrected ATN is expressed as

$$\text{corrected ATN} = \frac{\text{raw ATN}}{C \times R\,(\text{ATN})}. \quad (8)$$

We did not attempt to determine C in this study due to the lack of light absorption measurement by a reference method (e.g., the Multi-Angle Absorption Photometer or the photoacoustic spectrometer) (Schmid et al., 2006; Collaud Coen et al., 2010).

Compared to the reference values (i.e., those measured by the high-frequency denuded samples), both the ATN and EC results were biased low for the low-frequency samples, and moreover, the underestimation of EC (by about 15 %; Fig. 4) was more significant than ATN (by about 10 %; Fig. 5). Therefore, MAE calculated by Eq. (4) will appear to be higher for the low-frequency samples than the high-frequency ones. We do not present the detailed MAE results here, because in this study we are not able to reliably correct the ATN values retrieved from the carbon analyzer.

3.4 Effect of sampling frequency on the EC_R to EC_T ratio

In this section, OC and EC concentrations defined by the transmittance and reflectance charring correction will be referred to as OC_T and EC_T and OC_R and EC_R, respectively. The EC_R to EC_T ratio exhibited an apparent dependence on the abundance of OC defined by the OC_T to EC_T ratio (Fig. 6). The EC_R to EC_T ratio was close to 1.0 when the OC_T to EC_T ratio was relatively low, whereas with the increase of the OC_T to EC_T ratio, the EC_R to EC_T ratio first increased rapidly and then gradually approached an asymptotic value of about 2.0. This trend was independent of the sampling frequency. However, the majority of the EC_R to EC_T ratios appeared around the asymptotic value (i.e., ~ 2.0) for the low-frequency samples. Therefore, the discrepancy between EC_R and EC_T was more significant for the low-frequency samples (with an average EC_R to EC_T ratio of 1.91 ± 0.39) compared to the high-frequency ones (with an average EC_R to EC_T ratio of 1.56 ± 0.36).

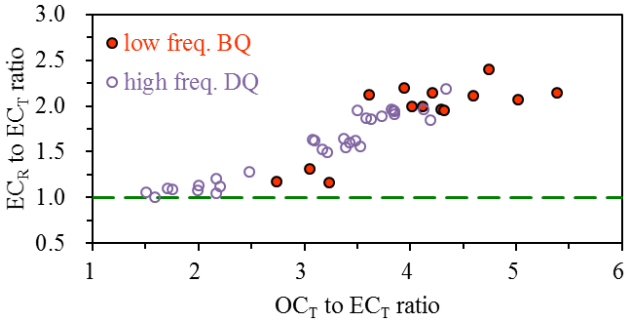

Figure 6. Dependence of the EC_R to EC_T ratio on the abundance of OC (estimated by the OC_T to EC_T ratio). The dashed line indicates an EC_R to EC_T ratio of 1.0. The EC_R and EC_T ratio averaged 1.91 ± 0.39 and 1.56 ± 0.36 for the low- and high-frequency samples, respectively; the difference is significant at a 95 % level of confidence (two-tailed $p = 0.005$).

4 Conclusions and implications

Carbonaceous aerosol in Beijing, China, was measured with different sampling configurations and frequencies. A major finding of this study is that the negative sampling artifact of a bare quartz filter could be remarkably enhanced due to the uptake of water vapor by the filter medium. It was also demonstrated that increasing sampling duration does not necessarily reduce the impact of positive sampling artifact. In addition, results from this study showed that with the increase of sampling duration, the analytical artifact was considerably enhanced such that EC concentrations of 48 h averaged samples were about 15 % lower than results from 24 h averaged ones and, meanwhile, both the EC_R vs. EC_T discrepancy and the shadowing effect in the determination of ATN became more significant.

Despite the limitations mentioned above, low-frequency sampling has its advantages, too, such as a lower cost for sampler operation and filter analysis, which may be attractive for large-scale and/or long period monitoring (e.g., by low-frequency sampling, $PM_{2.5}$ composition was measured for about 1 decade at an urban site in Beijing; Yang et al., 2011). Thus, low-frequency sampling may be a good choice when MEP decides to establish China's $PM_{2.5}$ speciation monitoring network. We suggest that if choosing low-frequency sampling, the flow rate should be carefully selected to reduce the negative sampling artifact and the analytical artifact (both of which are associated with filter loading).

The Supplement related to this article is available online at doi:10.5194/amt-8-2639-2015-supplement.

Acknowledgements. This work was supported by the National Natural Science Foundation of China (21307067 and 21190054) and by Tsinghua University under grant no. 20131089241. The first author was also supported by the International Postdoctoral Exchange Fellowship Program. We acknowledge Guenter Engling at the Desert Research Institute for revising and improving this paper.

Edited by: P. Herckes
Reviewed by: two anonymous referees

References

Boys, B. L., Martin, R. V., van Donkelaar, A., MacDonell, R. J., Hsu, N. C., Cooper, M. J., Yantosca, R. M., Lu, Z., Streets, D. G., Zhang, Q., and Wang, S. W.: Fifteen-year global time series of satellite-derived fine particulate matter, Environ. Sci. Technol., 48, 11109–11118, 2014.

Brown, A. S., Yardley, R. E., Quincey, P. G., and Butterfield, D. M.: Studies of the effect of humidity and other factors on some different filter materials used for gravimetric measurements of ambient particulate matter, Atmos. Environ., 40, 4670–4678, 2006.

Cavalli, F., Viana, M., Yttri, K. E., Genberg, J., and Putaud, J.-P.: Toward a standardised thermal-optical protocol for measuring atmospheric organic and elemental carbon: the EUSAAR protocol, Atmos. Meas. Tech., 3, 79–89, doi:10.5194/amt-3-79-2010, 2010.

Cheng, Y., He, K. B., Duan, F. K., Zheng, M., Ma, Y. L., Tan, J. H., and Du, Z. Y.: Improved measurement of carbonaceous aerosol: evaluation of the sampling artifacts and inter-comparison of the thermal-optical analysis methods, Atmos. Chem. Phys., 10, 8533–8548, doi:10.5194/acp-10-8533-2010, 2010.

Cheng, Y., Duan, F. K., He, K. B., Du, Z. Y., Zheng, M., and Ma, Y. L.: Intercomparison of thermal-optical method with different temperature protocols: implications from source samples and solvent extraction, Atmos. Environ., 61, 453–462, 2012.

Chiappini, L., Verlhac, S., Aujay, R., Maenhaut, W., Putaud, J. P., Sciare, J., Jaffrezo, J. L., Liousse, C., Galy-Lacaux, C., Alleman, L. Y., Panteliadis, P., Leoz, E., and Favez, O.: Clues for a standardised thermal-optical protocol for the assessment of organic and elemental carbon within ambient air particulate matter, Atmos. Meas. Tech., 7, 1649–1661, doi:10.5194/amt-7-1649-2014, 2014.

Chow, J. C., Watson, J. G., Crow, D., Lowenthal, D. H., and Merrifield, T.: Comparison of IMPROVE and NIOSH carbon measurements, Aerosol Sci. Technol., 34, 23–34, 2001.

Chow, J. C., Watson, J. G., Chen, L. W. A., Arnott, W. P., and Moosmüller, H.: Equivalence of elemental carbon by thermal/optical reflectance and transmittance with different temperature protocols, Environ. Sci. Technol., 38, 4414–4422, 2004.

Collaud Coen, M., Weingartner, E., Apituley, A., Ceburnis, D., Fierz-Schmidhauser, R., Flentje, H., Henzing, J. S., Jennings, S. G., Moerman, M., Petzold, A., Schmid, O., and Baltensperger, U.: Minimizing light absorption measurement artifacts of the Aethalometer: evaluation of five correction algorithms, Atmos. Meas. Tech., 3, 457–474, doi:10.5194/amt-3-457-2010, 2010.

de Jonge, D. and Visser, J. H.: PM gravimetric measurements and blank filters, European Aerosol Conference, 6–11 September, Karlsruhe, Germany, Abstract T200A01, 2009.

Eatough, D. J., Eatough, N. L., Pang, Y., Sizemore, S., Kirchstetter, T. W., Novakov, T., and Hobbs, P. V.: Semivolatile particulate organic material in southern Africa during SAFARI 2000, J. Geophys. Res., 108, 8479, doi:10.1029/2002JD002296, 2003.

Eck, T. F., Holben, B. N., Dubovik, O., Smirnov, A., Goloub, P., Chen, H. B., Chatenet, B., Gomes, L., Zhang, X. Y., Tsay, S. C., Ji, Q., Giles, D., and Slutsker, I.: Columnar aerosol optical properties at AERONET sites in central eastern Asia and aerosol transport to the tropical mid-Pacific, J. Geophys. Res., 110, D06202, doi:10.1029/2004JD005274, 2005.

He, X., Li, C. C., Lau, A. K. H., Deng, Z. Z., Mao, J. T., Wang, M. H., and Liu, X. Y.: An intensive study of aerosol optical properties in Beijing urban area, Atmos. Chem. Phys., 9, 8903–8915, doi:10.5194/acp-9-8903-2009, 2009.

Jathar, S. H., Farina, S. C., Robinson, A. L., and Adams, P. J.: The influence of semi-volatile and reactive primary emissions on the abundance and properties of global organic aerosol, Atmos. Chem. Phys., 11, 7727–7746, doi:10.5194/acp-11-7727-2011, 2011.

Kirchstetter, T. W., Corrigan, C. E., and Novakov, T.: Laboratory and field investigation of the adsorption of gaseous organic compounds onto quartz filters, Atmos. Environ., 35, 1663–1671, 2001.

Koch, D., Schulz, M., Kinne, S., McNaughton, C., Spackman, J. R., Balkanski, Y., Bauer, S., Berntsen, T., Bond, T. C., Boucher, O., Chin, M., Clarke, A., De Luca, N., Dentener, F., Diehl, T., Dubovik, O., Easter, R., Fahey, D. W., Feichter, J., Fillmore, D., Freitag, S., Ghan, S., Ginoux, P., Gong, S., Horowitz, L., Iversen, T., Kirkevåg, A., Klimont, Z., Kondo, Y., Krol, M., Liu, X., Miller, R., Montanaro, V., Moteki, N., Myhre, G., Penner, J. E., Perlwitz, J., Pitari, G., Reddy, S., Sahu, L., Sakamoto, H., Schuster, G., Schwarz, J. P., Seland, Ø., Stier, P., Takegawa, N., Takemura, T., Textor, C., van Aardenne, J. A., and Zhao, Y.: Evaluation of black carbon estimations in global aerosol models, Atmos. Chem. Phys., 9, 9001–9026, doi:10.5194/acp-9-9001-2009, 2009.

LaRosa, L. B., Buckley, T. J., and Wallace, L. A.: Real-time indoor and outdoor measurements of black carbon in an occupied house: an examination of sources, J. Air Waste Manage., 52, 41–49, 2002.

Liew, T. P. and Conder, J. R.: Fine mist filtration by wet filters – I. Liquid saturation and flow resistance of fibrous filters, J. Aerosol Sci., 16, 497–509, 1985.

Maimone, F., Turpin, B. J., Solomon, P., Meng, Q. Y., Robinson, A. L., Subramanian, R., and Polidori, A.: Correction methods for organic carbon artifacts when using quartz-fiber filters in large particulate matter monitoring networks: the regression method and other options, J. Air Waste Manage., 61, 696–710, 2011.

Malm, W. C., Schichtel, B. A., and Pitchford, M. L.: Uncertainties in $PM_{2.5}$ gravimetric and speciation measurements and what we can learn from them, J. Air Waste Manage., 61, 1131–1149, 2011.

McDow, S. R. and Huntzicker, J. J.: Vapor adsorption artifact in the sampling of organic aerosol: face velocity effects, Atmos. Environ., 24A, 2563–2571, 1990.

Müller, E. A., Rull, L. F., Vega, L. F., and Gubbins, K. E.: Adsorption of water on activated carbons: a molecular simulation study, J. Phys. Chem., 100, 1189–1196, 1996.

Panteliadis, P., Hafkenscheid, T., Cary, B., Diapouli, E., Fischer, A., Favez, O., Quincey, P., Viana, M., Hitzenberger, R., Vecchi, R., Saraga, D., Sciare, J., Jaffrezo, J. L., John, A., Schwarz, J., Giannoni, M., Novak, J., Karanasiou, A., Fermo, P., and Maenhaut, W.: ECOC comparison exercise with identical thermal protocols after temperature offset correction – instrument diagnostics by in-depth evaluation of operational parameters, Atmos. Meas. Tech., 8, 779–792, doi:10.5194/amt-8-779-2015, 2015.

Philip, S., Martin, R., van Donkelaar, A., Lo, J. W. H., Wang, Y. X., Chen, D., Zhang, L., Kasibhatla, P. S., Wang, S. W., Zhang, Q., Lu, Z., Streets, D. G., Bittman, S., and MacDonald, D. J.: Global chemical composition of ambient fine particulate matter for exposure assessment, Environ. Sci. Technol., 48, 13060–13068, 2014.

Piazzalunga, A., Bernardoni, V., Fermo, P., Valli, G., and Vecchi, R.: Technical Note: On the effect of water-soluble compounds removal on EC quantification by TOT analysis in urban aerosol samples, Atmos. Chem. Phys., 11, 10193–10203, doi:10.5194/acp-11-10193-2011, 2011.

Ram, K. and Sarin, M. M.: Absorption coefficient and site-specific mass absorption efficiency of elemental carbon in aerosols over urban, rural, and high-altitude sites in India, Environ. Sci. Technol., 43, 8233–8239, 2009.

Schauer, J. J., Mader, B. T., DeMinter, J. T., Heidemann, G., Bae, M. S., Seinfeld, J. H., Flagan, R, C., Cary, R. A., Smith, D., Huebert, B. J., Bertram, T., Howell, S., Kline, J. T., Quinn, P., Bates, T., Turpin, B., Lim, H. J., Yu, J. Z., Yang, H., and Keywood, M. D.: ACE-Asia intercomparison of a thermal-optical method for the determination of particle-phase organic and elemental carbon, Environ. Sci. Technol., 37, 993–1001, 2003.

Schmid, H., Laskus, L., Abraham, H. J., Baltensperger, U., Lavanchy, V., Bizjak, M., Burba, P., Cachier, H., Crow, D., Chow, J., Gnauk, T., Even, A., ten Brink, H.M., Giesen, K. P., Hitzenberger, R., Hueglin, C., Maenhaut, W., Pio, C., Carvalho, A., Putaud, J. P., Toom-Sauntry, D., and Puxbaum, H.: Results of the "carbon conference" international aerosol carbon round robin test stage I, Atmos. Environ., 35, 2111–2121, 2001.

Schmid, O., Artaxo, P., Arnott, W. P., Chand, D., Gatti, L. V., Frank, G. P., Hoffer, A., Schnaiter, M., and Andreae, M. O.: Spectral light absorption by ambient aerosols influenced by biomass burning in the Amazon Basin. I: Comparison and field calibration of absorption measurement techniques, Atmos. Chem. Phys., 6, 3443–3462, doi:10.5194/acp-6-3443-2006, 2006.

Solomon, P. A., Crumpler, D., Flanagan, J. B., Jayanty, R. K. M., Rickman, E. E., and McDade, C. E.: U.S. National $PM_{2.5}$ Chemical Speciation Monitoring Networks – CSN and IMPROVE: Description of networks, J. Air Waste Manage., 64, 1410–1438, 2014.

Subramanian, R., Khlystov, A. Y., Cabada, J. C., and Robinson, A. L.: Positive and negative artifacts in particulate organic carbon measurement with denuded and undenuded sampler configurations, Aerosol Sci. Tech., 38, 27–48, 2004.

Subramanian, R., Khlystov, A. Y., and Robinson, A. L.: Effect of peak inert-mode temperature on elemental carbon measured using thermal-optical analysis, Aerosol Sci. Tech., 40, 763–780, 2006.

ten Brink, H., Maenhaut, W., Hitzenberger, R., Gnauk, T., Spindler, G., Even, A., Chi, X., Bauere, H., Puxbaum, H., Putaud, J. P., Tursic, J., and Berner, A.: INTERCOMP2000: the comparability of methods in use in Europe for measuring the carbon content of aerosol, Atmos. Environ., 38, 6507–6519, 2004.

Turpin, B. J., Huntzicker, J. J., and Hering, S. V.: Investigation of organic aerosol sampling artifacts in the Los Angeles basin, Atmos. Environ., 28, 3061–3071, 1994.

Turpin, B. J., Saxena, P., and Andrews, E.: Measuring and simulating particulate organics in the atmosphere: problems and prospects, Atmos. Environ., 34, 2983–3013, 2000.

US EPA: Air Quality Criteria for Particulate Matter, EPA/600/P-99/002aF, Research Triangle Park, NC, 2004.

Viana, M., Chi, X., Maenhaut, W., Querol, X., Alastuey, A., Mikuška, P., and Večeřa, Z.: Organic and elemental carbon concentrations in carbonaceous aerosols during summer and winter sampling campaigns in Barcelona, Spain, Atmos. Environ., 40, 2180–2193, 2006.

Wang, S. X., Zhao, M., Xing, J., Wu, Y., Zhou, Y., Lei, Y., He, K. B., Fu, L. X., and Hao, J. M.: Quantifying the air pollutants emission reduction during the 2008 Olympic Games in Beijing, Environ. Sci. Technol., 44, 2490–2496, 2010.

Watson, J. G., Chow, J. C., Chen, L. W. A., and Frank, N. H.: Methods to assess carbonaceous aerosol sampling artifacts for IMPROVE and other long-term networks, J. Air Waste Manage., 59, 898–911, 2009.

Weingartner, E., Saathoff, H., Schnaiter, M., Streit, N., Bitnar, B., and Baltensperger, U.: Absorption of light by soot particles: determination of the absorption coefficient by means of Aethalometers, J. Aerosol Sci., 34, 1445–1463, 2003.

Yang, F., Tan, J., Zhao, Q., Du, Z., He, K., Ma, Y., Duan, F., Chen, G., and Zhao, Q.: Characteristics of $PM_{2.5}$ speciation in representative megacities and across China, Atmos. Chem. Phys., 11, 5207–5219, doi:10.5194/acp-11-5207-2011, 2011.

Yang, H. and Yu, J. Z.: Uncertainties in charring correction in the analysis of elemental and organic carbon in atmospheric particles by thermal/optical methods, Environ. Sci. Technol., 36, 5199–5204, 2002.

Zheng, B., Zhang, Q., Zhang, Y., He, K. B., Wang, K., Zheng, G. J., Duan, F. K., Ma, Y. L., and Kimoto, T.: Heterogeneous chemistry: a mechanism missing in current models to explain secondary inorganic aerosol formation during the January 2013 haze episode in North China, Atmos. Chem. Phys., 15, 2031–2049, doi:10.5194/acp-15-2031-2015, 2015.